Noname manuscript No.
(will be inserted by the editor)

Gershon Elber · Elaine Cohen

Probabilistic Silhouette Based Importance Toward Line-Art Non-Photorealistic Rendering

Abstract When pictorial information is presented, details of importance are typically emphasized. These include discontinuities in the geometry, highly curved regions, silhouettes, etc.

This work analyzes the probability that certain smooth surface regions or polygonal edges possess silhouettes. This probability analysis is then associated with the visual importance of the local neighborhood, which is capable of capturing discontinuities and highly curved regions.

A non-photorealistic rendering technique is subsequently proposed to take advantage of the silhouette-based importance. Based on this importance analysis, we present a completely automatic algorithm that creates line-art that captures visual features in the model in an appealing way.

Key Words: Silhouettes, NPR rendering, Gaussian Sphere, Visibility Determination, Feature and Suggestive Contours.

1 Introduction

Silhouette curves play a major role in many non-photorealistic (NPR) line drawings. Since silhouette curves provide intuitive cues to the shape of an object, a large body of research has been devoted toward efficient and accurate extraction of such curves. Algorithms have been presented to extract silhouette curves from polygonal meshes [1,12,14,18], parametric freeform surfaces [8], implicit freeform surfaces [2,16] and even iso-surfaces of volumetric data sets [13,21].

Gershon Elber
Computer Science Department
Technion, Israel
Email: gershon@cs.technion.ac.il

Elaine Cohen
Computer Science Department
University of Utah, SLC, Utah, USA
Email: cohen@cs.utah.edu

The search for silhouette edges of a polygonal model can be exhaustive. It may require searching all the front-facing polygons in a model for back-facing neighbors or vice versa. This test is a time-consuming task that is linear in the number of polygons n, whereas, in general, a polygonal model approximating a C^1 continuous geometry with n polygons will present only $\sqrt{n}$ silhouette edges [1]. In [1,17], output-sensitive algorithms that approach $O(m)$ time complexity, where m represents the size of the output or the number of silhouette edges, were presented for orthographic and perspective views, respectively. Markosian et al. [14] presented a probabilistic algorithm that randomly examines whether edges in the model are silhouettes. Once a silhouette edge is detected, the algorithm serves as a seed for tracing the silhouette curve along the polygonal model. This algorithm does not guarantee that all silhouettes will be found but the longer the silhouette curve is, the greater the likelihood of its being detected.

Image-based extraction of silhouette edges [18,20] is becoming popular due to the availability of graphics rendering hardware (GPUs) that enables extraction of silhouette curves in real time. Image processing is employed to detect locations at which front and back facing polygons share the same depth; that is, along the silhouettes.

Extraction of silhouettes from freeform surfaces is typically performed either by tessellating the freeform shape into polygons and using one of the methods discussed above or by fetching the silhouette edges directly from the surface. Let $S(u,v)$ be a regular C^1 rational parametric surface and let V be the viewing direction. The silhouette curves can now be characterized via the following rational constraint:

$$\left\langle \frac{\partial S(u,v)}{\partial u} \times \frac{\partial S(u,v)}{\partial v}, V \right\rangle = 0. \tag{1}$$

In general, the solutions for Equation (1) can be found only numerically. Alternatively, divide-and-conquer subdivision algorithms can be used [8]. Tracing the silhouette curves on the surfaces is common for implicit representation solutions.

While the body of silhouette extraction methods is large, the converse, as presented below, is rarely investigated:

Query 1 *What is the probability of a small surface region (a polygon edge) containing (being) a silhouette, given an arbitrary viewing direction?*

Answering Query 1 should shed some light on the *visual importance* of this small region or edge. Because silhouette curves are visually important, we expect that regions (edges) with a high probability of containing (serving as) silhouettes will also be visually important.

A goal of this research is to quantify the visual importance of surface regions based on a *probabilistic silhouette analysis* for both polyhedra and continuous freeform geometry. The potential importance of the dihedral angle between adjacent polygons has been recognized in the past; for a recent example, see [22]. In [14], the edges of the model are sorted based on their dihedral angle, so as to increase the probability of finding the silhouette edges. Interestingly enough, the claim was made in [14], without proof, that the probability of an edge to be a silhouette is proportional to $\pi - \theta$ where θ is the dihedral angle in radians. Theorem 1 in the next section substantiates this claim and makes it more precise.

Silhouettes curves are considered important because they convey a shape's visual cues. However, they can fail to provide significant shape cues when crucial features are all front- (or all back-) facing. For example, consider looking at a human face head on. Very few, if any, silhouette curves would be visible from this specific perspective. Researchers who recognized this drawback have searched for ways to augment the silhouette drawings with other curves or contours that provide more information about the shape. For example, [23] examined a combination of silhouette curves, boundary curves, creases that depicts folds and convex and concave regions.

Curvature properties, such as lines of curvature [11], have been examined as "feature-strokes" but the visual cues they provide are not always as intuitive as silhouette curves. While lines of curvature might nicely portray the local shape of the geometry, they can also be confusing, for example, along umbilicals. Further, since lines of curvature are defined along the entire geometry, they do not capture significant geometry such as that of creases or ridges. This vital geometry could be sought at the extremum locations of the principal curvature while moving along the line of curvature. This approach to the computation of creases was used in [24] for registration of volumetric data sets, and might be helpful in NPR applications as well.

Other attempts to exploit curvature properties include the use of parabolic lines [9], or locations on the surface where the Gaussian curvature vanishes. While parabolic lines are intrinsic to the geometry, they are also very sensitive to noise. Small perturbations of the geometry, especially if the geometry is *almost* developable, are liable to produce great changes in the parabolic set. Recently, curvature-based feature lines were sought in the context of non-photorealistic rendering [3]. Zeros of the normal curvature in the direction of a projection of the view direction onto the tangent plane, denoted as the radial curvature, were suggested as features of interest. This approach of [3] examined the possibility of having silhouettes under a small perturbation of the viewing direction and is closely associated with the extraction of parabolic locations.

Second order differential properties, such as lines of curvatures and radial curvatures, and third order differential properties that are needed to detect creases, may be difficult and numerically unstable to compute, especially for piecewise linear polygonal meshes. In this work, we show that one can go a long way in detecting features of visual importance with first order analysis of polygonal meshes, taking full advantage of a probabilistic silhouette analysis. Herein, all features, either soft, rounded or sharp, are captured by conducting a global silhouette viewing analysis.

The rest of this work is organized as follows. In Section 2, a probabilistic analysis of silhouette curves is carried out for both polygonal and freeform parametric geometry. In Section 3, we make a general importance texture map that can be used in any rendering scheme, continuously prescribing the important surface regions. We then demonstrate its possible use in line-art NPR renderings. In Section 4, we present some examples and finally, we conclude in Section 5.

2 Silhouettes and Visual Importance

As silhouette curves will play a major role in our forthcoming discussion, we give an outline of the essence of silhouette curves. Consider a C^1 continuous surface and let V be the viewing direction. Then,

Definition 1 Point $P \in S(u, v)$ is a *silhouette point* if the normal to the surface at P, N, is orthogonal to V, i.e. $\langle N, V \rangle = 0$.

We propose an approach for the enhancement of features in NPR-based rendering by analyzing their importance, for both the discrete (polygonal) and continuous domains. Let V be a point on the unit sphere, S^2. V will denote one random viewing direction out of all possible viewing directions, or points on S^2. We define the *importance* of a surface region as follows.

Definition 2 The *importance* of a region (an edge) is measured by its probability of containing (being) a silhouette from a random viewing direction V.

This probabilistic view will take into account sharp corners as well as emphasize continuous surface regions that are highly curved, and hence have a high probability

of being or containing a silhouette. As a result, looking at a human face head on, highly curved creases and ridges are likely to be emphasized even if they do not form silhouettes from the current view direction.

In Section 2.1, the probabilistic silhouette visibility model for polygonal meshes is explored and defined whereas in Section 2.2 continuous freeform surfaces are considered.

2.1 Silhouette Importance in Polygonal Meshes

Let F_i and F_j be two faces of a polygonal mesh sharing an edge E_{ij}, and let α_{ij} be the angle between the two normals N_i (of F_i) and N_j (of F_j). Assume angles are measured in radians. Then,

Theorem 1 *The probability, p_{ij}, that edge E_{ij} is a silhouette edge in an orthographic projection and an arbitrary viewing direction V is*

$$p_{ij} = \frac{\alpha_{ij}}{\pi}.$$

Proof: Assume N_i and N_j point outward from the model. Face F_i (F_j) is visible from a hemisphere, H_i (H_j), of viewing directions,

$$H_i = \{V \mid \langle N_i, V\rangle \leq 0\}\, (H_j = \{V \mid \langle N_j, V\rangle \leq 0\}).$$

In order for E_{ij} to be a silhouette edge, only one face should be visible. Then, V is part of H_i but not of H_j, or alternatively part of H_j but not of H_i. Therefore, the probability that E_{ij} is a silhouette edge equals the probability that V will be contained in a symmetric difference of H_i and H_j, $(H_i - H_j) \cup (H_j - H_i)$, divided by the area of the entire unit sphere; see Figure 1.

Without loss of generality, assume N_i and N_j are both in the $Z = 0$ plane. Then, every cross-section of the unit sphere with a plane $P : Z = Z_0$ will result in a complete circle and two arcs, $(H_i - H_j) \bigcap P$ and $(H_j - H_i) \bigcap P$, of α_{ij} radians each. Put differently, $2\alpha_{ij}$ radians of every such circular cross-section are covered by $(H_i - H_j) \cup (H_j - H_i)$. Therefore, $\frac{2\alpha_{ij}}{2\pi}$ of each circular cross-section is covered.

Because the circles can form a differential to be integrated into the area of the sphere, $\frac{2\alpha_{ij}}{2\pi}$ of the area of the sphere is covered by $(H_i - H_j) \cup (H_j - H_i)$.
■

2.2 Silhouette Importance for Freeform Surfaces

Let $S(u, v)$ be a C^1 continuous freeform parametric surface with finite Lipschitz conditions. Direct application of Theorem 1 to a freeform surface $S(u, v)$ fails since a single point on a C^1 continuous $S(u, v)$ surface has zero probability of being on a silhouette curve! This can be explained by the fact that at the limiting neighborhood of this point, the normal to the surface does not change due to the C^1 continuity and the Lipschitz conditions.

Instead, one needs to consider a small region of the surface and seek the probability that a silhouette curve goes through some differential area element dA of $S(u, v)$. Assume such a small differential surface element with domain $[u_0, u_1]$, $[v_0, v_1]$ exists. Consider the four unit normals at the four corners of dA, $N_{i,j} = N(u_i, v_j)$, $i, j = 0, 1$. In the limit, these four normals bound the normal deviation of dA. Examine the differential Gauss map, dG, of dA on the unit sphere S^2. We assume that the normals deviate linearly along the boundary of dG and hence connect the boundaries as great arcs on the Gaussian sphere S^2. This assumption holds in the limit when dA vanishes; see Figure 2.

The following definition is derived from Definition 1:

Definition 3 The surface region dA contains a silhouette curve from direction V if there exists a normal $N \in dG$ such that $\langle V, N\rangle = 0$.

Consider the set $\mathcal{V} \subset S^2$ of all viewing directions on S^2 for which dA has a silhouette,

$$\mathcal{V} = \{V \mid \exists N \in dG \text{ such that } \langle V, N\rangle = 0\},$$

and let $|\mathcal{V}|$ denote the area of $\mathcal{V}$. Thus we can say:

Theorem 2 *Let H_{ij} be the hemisphere of visibility associated with normal $N_{i,j}$, $i, j = 0, 1$, the four normals prescribing region dG. Then, the probability, p_{dA}, that differential surface area element dA will present a silhouette equals*

$$p_{dA} = \frac{|\mathcal{V}|}{4\pi} = \frac{\bigcup_{i,j=0,1} H_{i,j} - \bigcap_{i,j=0,1} H_{i,j}}{4\pi}, \tag{2}$$

where $|\mathcal{V}|$ denotes the area of $\mathcal{V}$.

Proof: We assume that the four boundaries of dG are great arcs. Then, for dA to present a silhouette from V, the following must hold:

$$\langle V, N_{i,j}\rangle \langle V, N_{l,m}\rangle < 0,$$

for some $i, j, l, m = 0, 1$. Examine the complement. If either $\langle V, N_{i,j}\rangle > 0$, $\forall i, j = 0, 1$, or $\langle V, N_{i,j}\rangle < 0$, $\forall i, j = 0, 1$, dA presents no silhouettes from V.

However, $\langle V, N_{i,j}\rangle > 0$, $\forall i, j = 0, 1$ if and only if $V \in \bigcap_{i,j=0,1} H_{i,j}$. Similarly, $\langle V, N_{i,j}\rangle < 0$, $\forall i, j = 0, 1$ if and only if $V \notin \bigcup_{i,j=0,1} H_{i,j}$. Hence, V presents a silhouette in dA if and only if it is in the union of the four hemispheres (see Figure 3 (a)) but is not in the intersection of the four hemispheres. In Figure 3 (a), the intersection and the union of these four hemispheres are shown as a thin black line.

Therefore, the probability that dA presents a silhouette is the same as the area of the strip on S^2, $|\mathcal{V}| = \bigcup_{i,j=0,1} H_{i,j} - \bigcap_{i,j=0,1} H_{i,j}$ divided by the entire area of S^2.
■

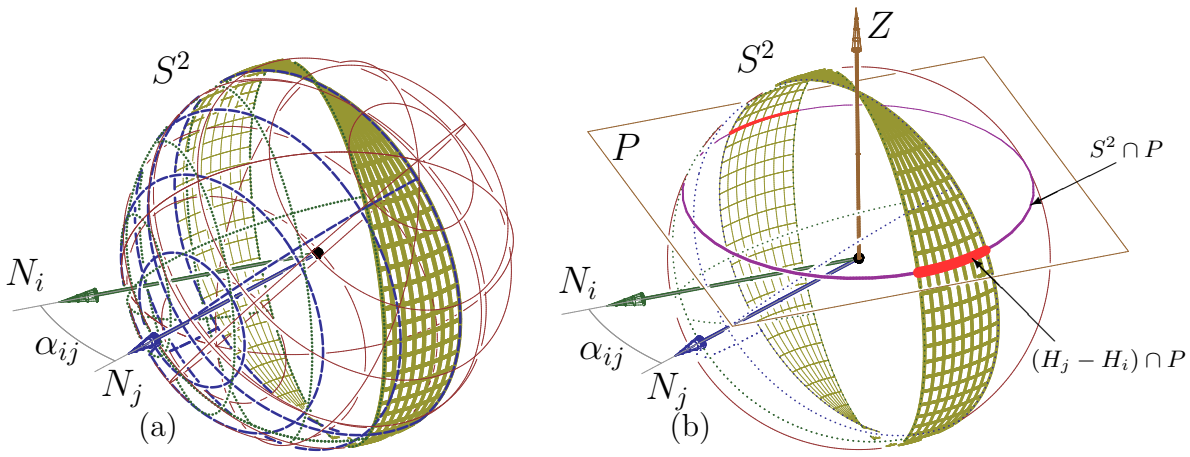

Fig. 1 In (a), two normals on the Gaussian sphere S^2, N_i and N_j, of two polygons F_i and F_j sharing an edge E_{ij}, are each visible from hemispheres of directions H_i (green) and H_j (blue), centered around N_i and N_j, respectively. Edge E_{ij} is a silhouette from viewing direction V if and only if $V \in (H_i - H_j) \cup (H_j - H_i)$. The $(H_i - H_j) \cup (H_j - H_i)$ region is marked by thick yellow lines. In (b), a horizontal circular cross-section (magenta) of S^2 with a plane $P : Z = Z_0$ shows that the relative coverage (red) of $(H_j - H_i) \bigcap P$ is proportional to $\frac{\alpha_{ij}}{\pi}$.

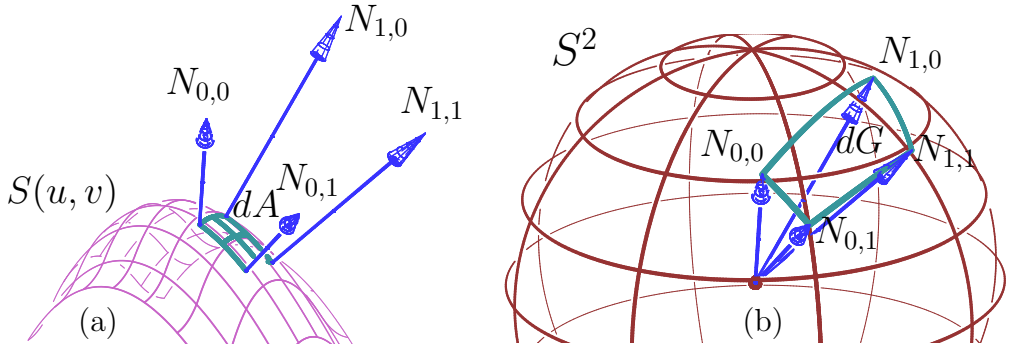

Fig. 2 In (a), a differential area element dA (cyan) of surface $S(u, v)$ is examined. In (b), the corresponding region of the Gauss map of dA (also cyan) is marked on the Gaussian sphere S^2 as dG.

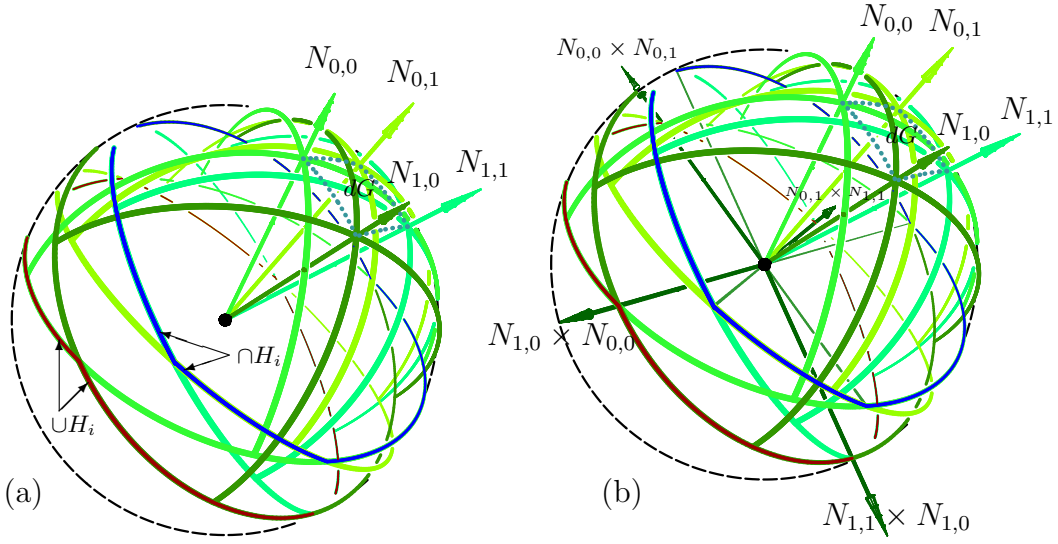

Fig. 3 Surface region dA and its Gauss map dG (dotted cyan) present a silhouette from V if and only if V is in the strip on the Gauss map between $\bigcup H_i$ (red) and $\bigcap H_i$ (blue) (a). The two boundaries of this strip are defined by four great arcs through vectors $N_{i,j} \times N_{l,m}$ and their antipodal vectors (b).

The boundary of $\bigcup_{i,j=0,1} H_{i,j}$ is in fact the antipodal set of the boundary of $\bigcap_{i,j=0,1} H_{i,j}$, on S^2. This is evident from the fact that the union of the hemispheres of vectors V_i shares the same boundary as the intersection of the hemispheres of vectors $-V_i$. The computation of either $\bigcup_{i,j=0,1} H_{i,j}$ or $\bigcap_{i,j=0,1} H_{i,j}$ is not straightforward and is beyond this paper. Nonetheless, one can show that Equation (2) is equal to

$$p_{dA} = \frac{2\delta(||N_v|| + ||N_u||))}{\pi}, \tag{3}$$

where $||N_u||$ and $||N_v||$ are the magnitudes of the partials of the unit normal field with respect to u and v and $\delta \in \mathbb{R}^+$ prescribes the size of the differential area dA.

This result deserves some discussion. While, at first glance, Equation (3) might look unbounded and hence could yield results larger than one, this equation computes ratios of areas over the sphere and hence can never exceed the value of one. In addition, Equation (3) is linearly dependent on δ, the size of the surface region being considered. In other words, the probability of a surface region possessing a silhouette linearly depends on the size of the region.

It is well known that the ratio of the areas of dG and dA equals the Gaussian curvature, K, of S, in the limit [5]. Yet, K fails to measure the probability that a surface region contains a silhouette. For any developable region, K is identically zero, and hence the area of dG is zero. Yet, any region of finite area in a cylinder, dA, has a finite probability of being a silhouette. The measure portrayed in Equation (3) takes into account the lengths of the boundary edges of dG, $||N_v||$ and $||N_u||$. While one of them can vanish for a general developable surface, both will vanish only if the surface is planar - indeed, a case with zero probability of having a silhouette.

We conclude this section with one final remark. Result (3) is closely related to the Milner form of the Cauchy-Crofton formula [5] on a sphere that directly relates the probability that a great circle intersects a curve on S^2, possibly more than once, with its length. Here the probability of a great circle intersecting a boundary of dG (which is a great arc and hence can intersect a great circle at most once) amounts to having a silhouette cross the corresponding boundary curve of region dG.

Being able to compute the probability of an edge in a polygonal mesh or a surface region to possess a silhouette, we can now propose an algorithm, in Section 3, that takes advantage of this ability for line-art NPR rendering.

3 Line-art NPR Rendering Using Importance Maps

In Section 2, we established a way to derive the probability of a surface region or an edge possessing a silhouette. Clearly, one can define an importance map for the surfaces of the object and use these maps to guide any further rendering scheme, photorealistic or not.

For a continuous surface domain, the importance function is defined everywhere and could be derived following Section 2.2. In the discrete case, we get a measure of importance for the edges when we follow Section 2.1. Clearly, one can set the importance of a triangle to depend on the importance of its three edges. This can be the edge with the maximal importance or the average of the importance of the three edges of the triangles. In this work, we have chosen to employ the average of the edges.

Having set the importance map of the model, one can spread $\sim n$ seed points with a distribution that is influenced by this importance map. Sharp corners or highly curved continuous regions will be marked high on the importance map and hence will attract more seed points. Compute the total area of the model, $\mathcal{A}$, and for each triangle, T_i, in the model, of area $\mathcal{A}_{T_i}$, distribute $\mathcal{I}_{T_i} n \mathcal{A}_{T_i}/\mathcal{A}$ points over T_i, normalized by the estimated importance of the triangle, $\mathcal{I}_{T_i}$. Let V_1, V_2, V_3 be the three vertices of triangle T_i and consider vectors $V_{12} = V_2 - V_1$ and $V_{13} = V_3 - V_1$. Then, the position of seed point $P^s \in T_i$ is set to

$$P^s = \begin{cases} V_1 + V_{12}\alpha + V_{13}\beta, & \alpha + \beta \leq 1, \\ V_1 + V_{12}(1-\alpha) + V_{13}(1-\beta), & \alpha + \beta > 1, \end{cases}$$

where α and β are two independent, uniformly distributed random numbers between zero and one. $V_1 + V_{12}\alpha + V_{13}\beta$ is contained in the parallelogram spanned by V_{12} and V_{13}. Hence, to ensure $P^s \in T_i$, seed point P^s is reflected along edge $\overline{V_2V_3}$ if $\alpha+\beta > 1$, as $P^s = V_1+V_{12}(1-\alpha)+V_{13}(1-\beta)$.

¿From these seed points, line strokes are grown by marching on the surface along prescribed directions. Starting from a seed point, $P_i^s = (p_i^x, p_i^y, p_i^z)$, the next position is calculated by computing the intersection of the forward stroke's direction and the boundary of the current triangle. This process continues until the accumulated length of the stroke exceeds its prescription. Possible options for strokes' directions are (see Figure 4 for a rendering of the strokes near the silhouette regions):

- Isoclines or isophotes [10] on $\mathcal{O}$ or lines of constant inclination of the normal with respect to the view or light source directions (see Figure 4 (a)). Given a direction V, inclination angle γ, and an edge, E_{ij}, with vertices V_i and V_j with two end normals N_i and N_j, we seek the solution, if any, to

  $$t\,\langle N_i, V\rangle + (1-t)\,\langle N_j, V\rangle = \cos(\gamma), \quad t \in [0,1].$$

- Orthoclines on $\mathcal{O}$ or curves orthogonal to the isoclines (see Figure 4 (b)). Traditionally, shaded regions are sketched with strokes that break the regularity of the edge between the illuminated and shaded regions. Since the isoclines, by definition, will align themselves in parallel to this shadow-illumination border, the orthoclines are natural candidates to sketch shaded domains, breaking this regularity.

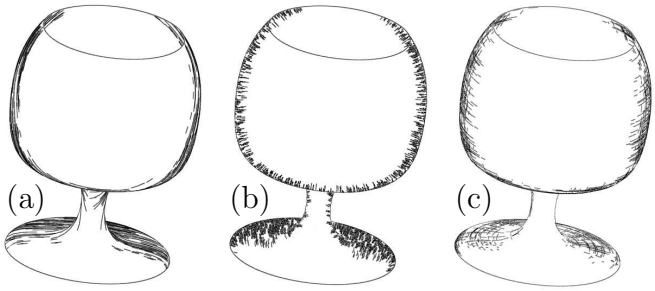

Fig. 4 A simple wine glass model is rendered with strokes along isoclines (a), along orthoclines (b) and along lines of curvature (c). Note these strokes are not following any importance information and are rendered along silhouette regions.

Algorithm 1: *Silhouette importance based line-art NPR*
Input:
Object $\mathcal{O}$, a polygonal mesh;
Output:
Silhouette importance based line-art NPR rendering of $\mathcal{O}$;
Algorithm:
SilImpNPR2($\mathcal{O}$)
begin
$\mathcal{I}_{E_i} \Leftarrow$ *Importance of all edges* E_i *in* $\mathcal{O}$;
$\mathcal{I}_{T_j} \Leftarrow$ *Importance of all triangles* T_j *in* $\mathcal{O}$, *derived as average or maximum over adjacent edges to* T_j;
$\mathcal{P} \Leftarrow$ *random seed points on* $\mathcal{O}$ *with a distribution that is based on the triangles' importance map;*
For each seed point $P_i^s \in \mathcal{P}$ *do*
begin
$\mathcal{S}_i \Leftarrow$ *stroke(s) grown from* P_i^s *over* $\mathcal{O}$;
end
Output $\{\mathcal{S}_i\}$;
end.

– Lines of curvature [6,11,19] on $\mathcal{O}$ (see Figure 4 (c)). Here, in the discrete polygonal case, a local paraboloid fit is computed at the neighborhood of a vertex V or location P [15], only to fetch the two principal directions on $\mathcal{O}$ at V or P. These two directions are then intersected with the edges of the triangle.

For more details on the way we compute the strokes over the geometry, set and select the strokes geometry and length, see [6]. Algorithm 1 summarizes this process.

4 Examples

In this section, we present some examples that use silhouette based importance toward NPR renderings. All the presented examples were created using the IRIT solid-modeling environment [7]. We believe that the combination of view-independent features such as the silhouette based importance scheme presented here, with view-dependent information such as shading and silhouettes is the key to a successful creation of NPR drawing. In this section, examples of these different components as well as the combined final result are presented. To give a bit more intuition to the silhouette based importance map, Figure 5 is presented. The dinosaur in Figure 5 is colored according to the value of the silhouette based importance map from green through blue to red.

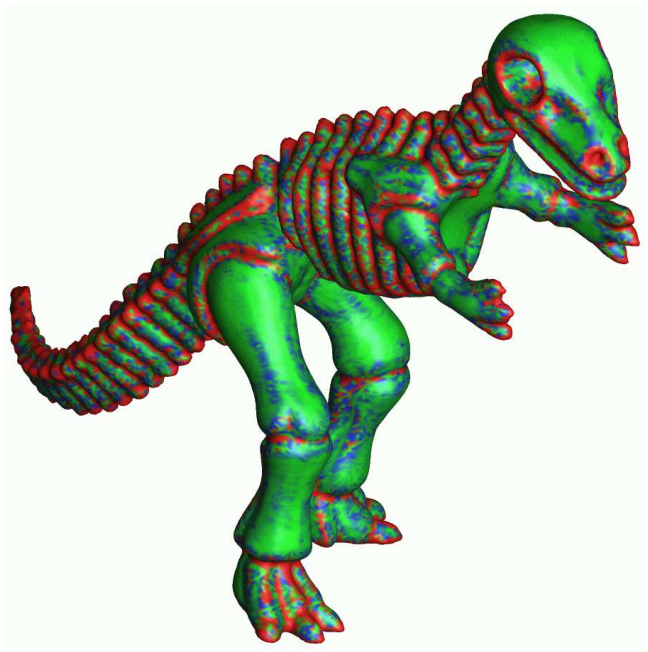

Fig. 5 A model of a dinosaur is rendered with colors coded following the silhouette based importance map. See also Figure 7.

In Figure 6, Algorithm 1 is combined with cosine shading information. In Figure 6 (a), the result of using only silhouette edges are shown whereas in Figure 6 (b), the importance is evaluated using Algorithm 1 and importance strokes are rendered along isoclines. In Figure 6 (c) both the importance (as in Figure 6 (b)) and cosine shading strokes along orthoclines are combined together.

Figure 7 demonstrates several levels of importance thresholding. Figure 7 (a) presents the model with only silhouettes, whereas Figures 7 (b) to (d) show three threshold levels of importance strokes. In Figure 7, strokes along lines of curvature are employed.

The Stanford model of the David status is shown in Figures 8 and 9. In Figure 8, the full statue is presented with silhouette only drawings (Figure 8 (a)), and cosine shading orthocline strokes and silhouettes (Figure 8 (b)). The result of using isocline importance strokes is shown in Figure 8 (c), and as an image with both isocline importance strokes and orthocline cosine shading strokes (Figure 8 (d)). In Figures 9 (a) and (b), the importance map that is derived with the aid of Algorithm 1 is used to generate isocline strokes. In Figure 9 (c), the head is rendered with additional orthocline cosine shading strokes.

Figures 10 and 11 present a few more complete drawings. In Figure 10, two models, a toy pony and a tri-

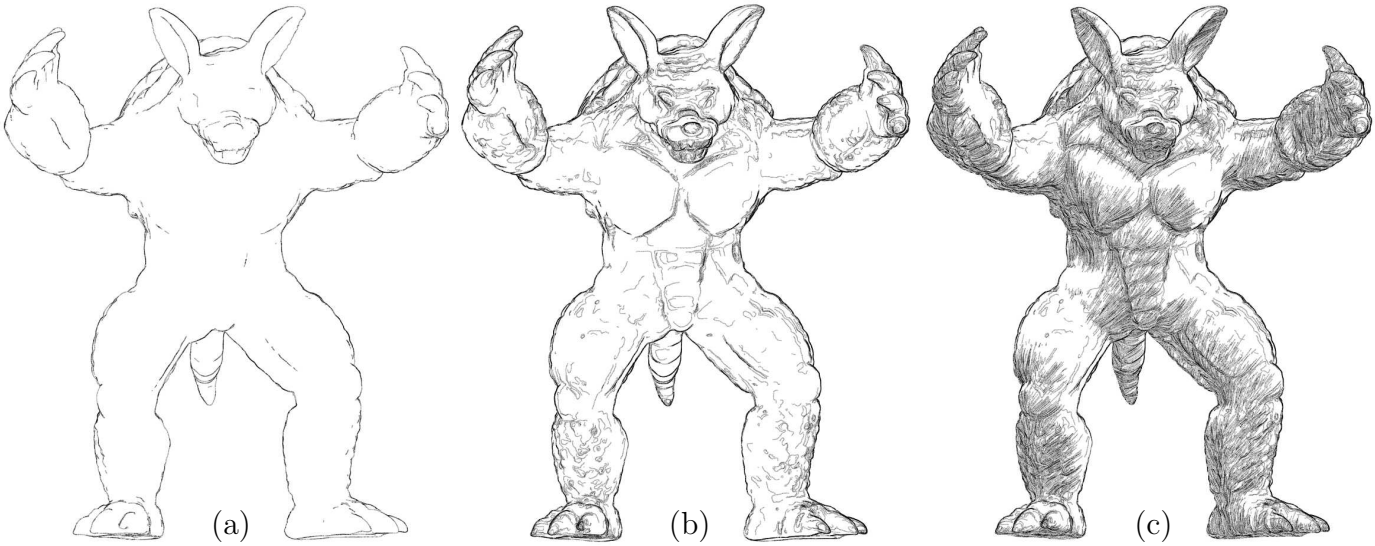

Fig. 6 The armadillo model is rendered using silhouettes only in (a) and using the importance algorithm, Algorithm 1, and isoclines importance strokes in (b). (c) presents the combined image of both the importance isoclines and shaded orthocline strokes.

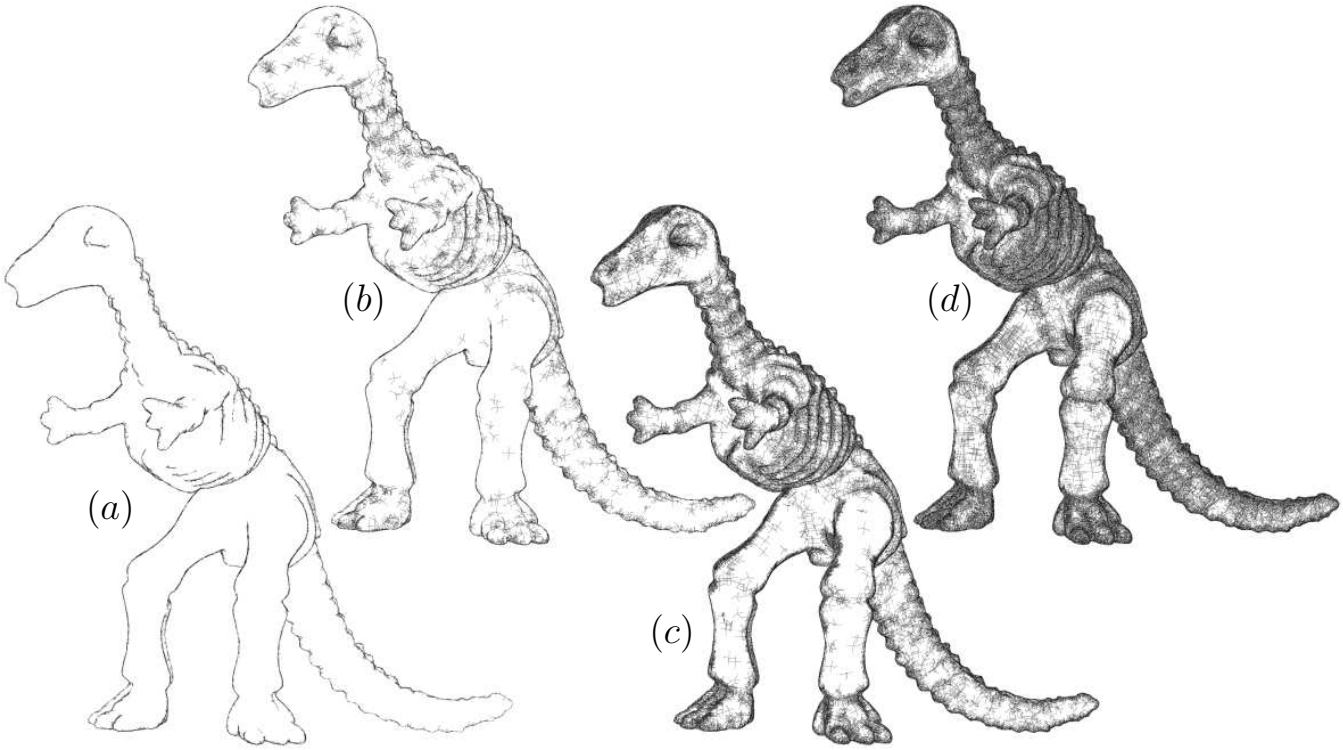

Fig. 7 A model of a dinosaur is rendered using silhouettes only (a), and using Algorithm 1 in (b)-(d). (b) and (d) present different levels of thresholding the importance values as computed over the polygonal mesh. Note, for example, the progressive appearance of the knee joints. The presented strokes are oriented along lines of curvature. See also Figure 5.

cycle, are presented whereas in Figure 11, two anatomical renderings of a human foot and torso are presented. All drawings include importance rendering using isoclines with respect to the view direction and cosine shading using orthoclines from the direction of the light source.

Finally, Figure 12 presents two examples of directly rendered NURBs surfaces using a parametric surface variant of Algorithm 1, computing the importance map following Section 2.2. The dinner scene in Figure 12 (a) contains around forty NURBs surfaces, mostly bi-cubic and

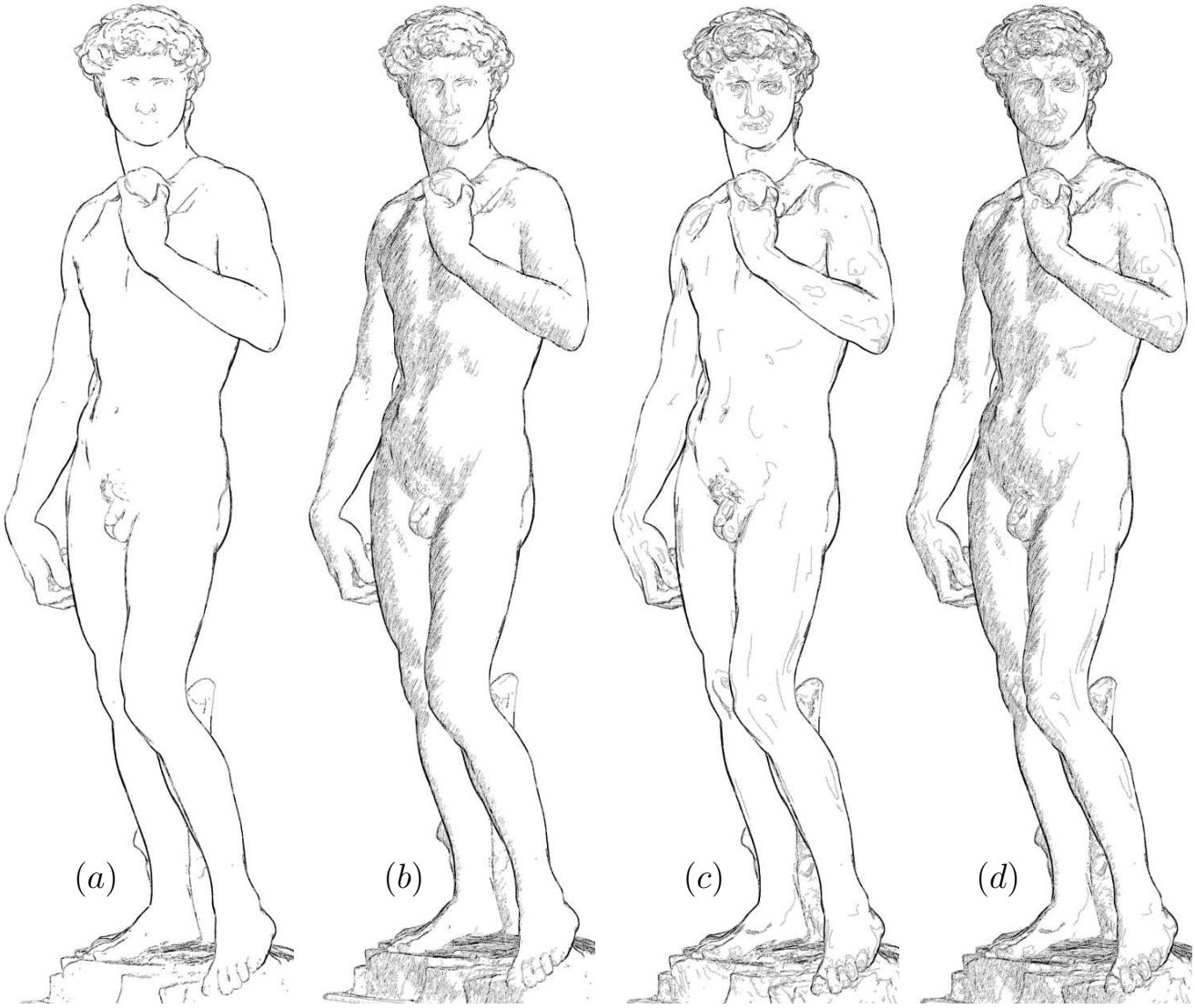

Fig. 8 The full David statue is rendered using silhouettes only in (a), and using cosine shading orthocline strokes and silhouettes in (b). In (c), the statue is rendered using the importance map of Algorithm 1 and isocline strokes. Finally, (d) presents a composition of both importance isocline strokes and cosine shading orthocline strokes.

bi-quadratic. Note the transparency effect that is gained for the glassware by ignoring these artifacts in the Z-buffer. The mask surface in Figures 12 (b) and (c) is a single bi-cubic surface with around 2500 (50×50) control points. The images were rendered with orthocline cosine shading strokes and isocline importance strokes.

All the images presented in this work were created in a few seconds once the strokes were computed, on a modern PC. The strokes' computation took from a fraction of a second in simple cases to a few dozen seconds in a highly detailed model that used lines of curvatures-based strokes.

5 Discussion and Conclusion

In this work, we have investigated the global probability of an edge of a polygonal mesh or a small region of a freeform smooth shape possessing a silhouette. We further exploited this probability as an importance measure for that neighborhood and considered a completely automatic line-art NPR algorithm that takes advantage of this importance map.

The view-dependent approach proposed by [3] faces difficulties in regions with no cavities. Since contours move in [3], a stabilization solution must be derived before using that approach in animations. In contrast, our work performs a global, view-independent analysis that performs equally well in all cases, concave or not, and finds the geometrically intrinsic feature location. The presented

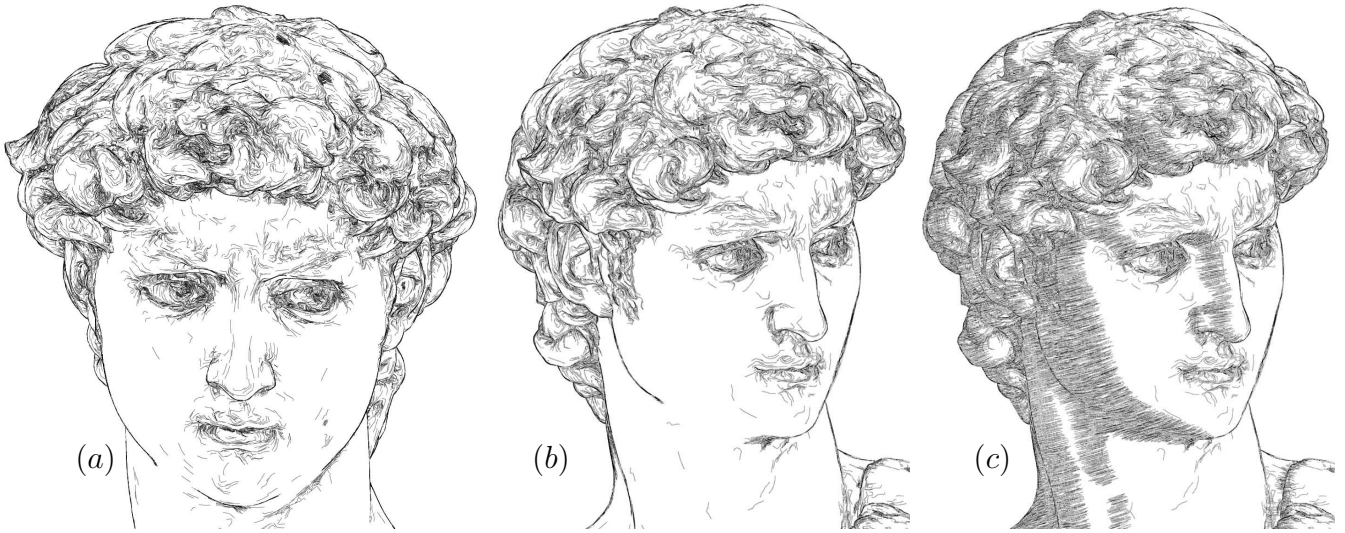

Fig. 9 The David's head is rendered using Algorithm 1 in (a) and (b), showing the importance using the isoclines' strokes. In (c), shaded strokes are computed and added to (b), as orthoclines.

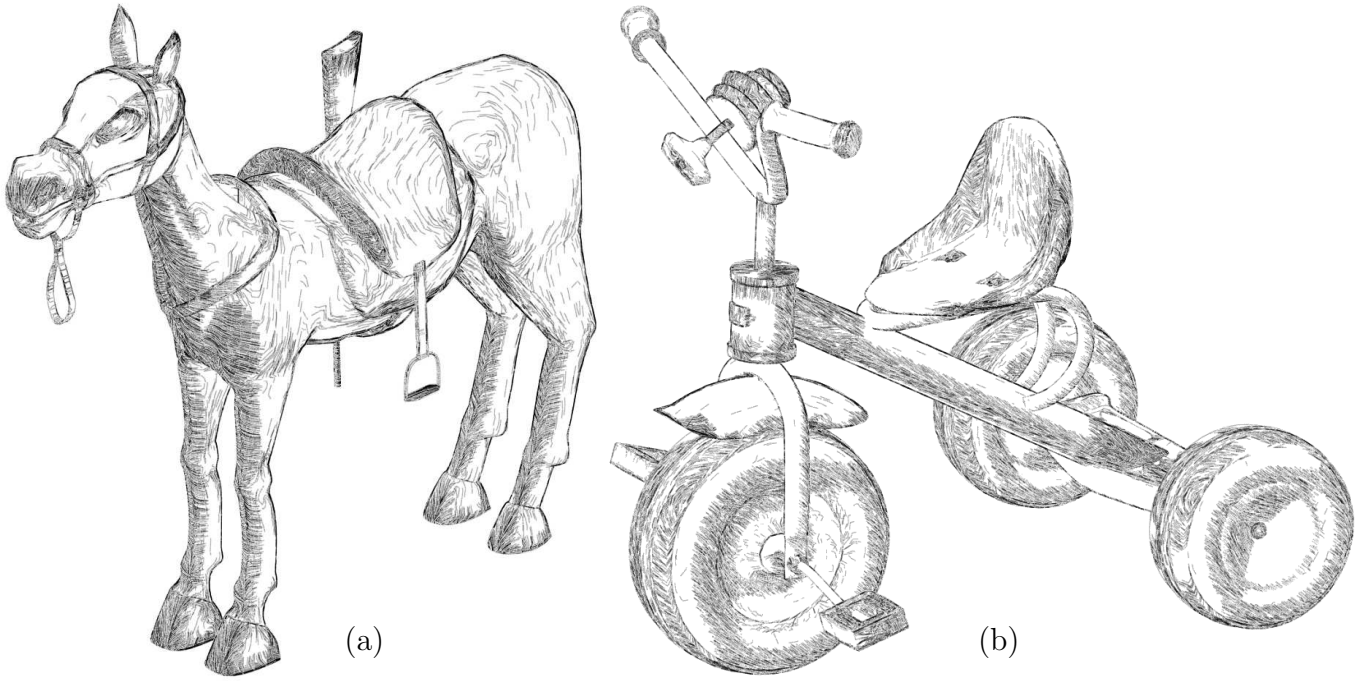

Fig. 10 Models of a tricycle (a) and a toy pony (b) rendered with the aid of Algorithm 1, with orthocline cosine shading strokes and isocline importance strokes.

importance map ranks all detected features in a continuous manner. As a result, features are never missed, and sharp features are smoothed out. Thresholding the importance map might allow one to emphasize a few crucial features. Additional analysis of the properties of this continuous importance map is probably in order. Nevertheless, this view-independence ability makes the presented approach a prime candidate for animation and our preliminary examination indeed shows this.

The approach presented herein is stable. Notwithstanding, it should probably be integrated with and augmented by other feature extraction and shape measuring methods, especially those that capture sharp features, such as the various existing second and third order differential analysis tools [3, 11, 23, 24].

Because large umbilical regions, such as spheres or planes, will present constant importance and hence will be identically emphasized, any importance map must be

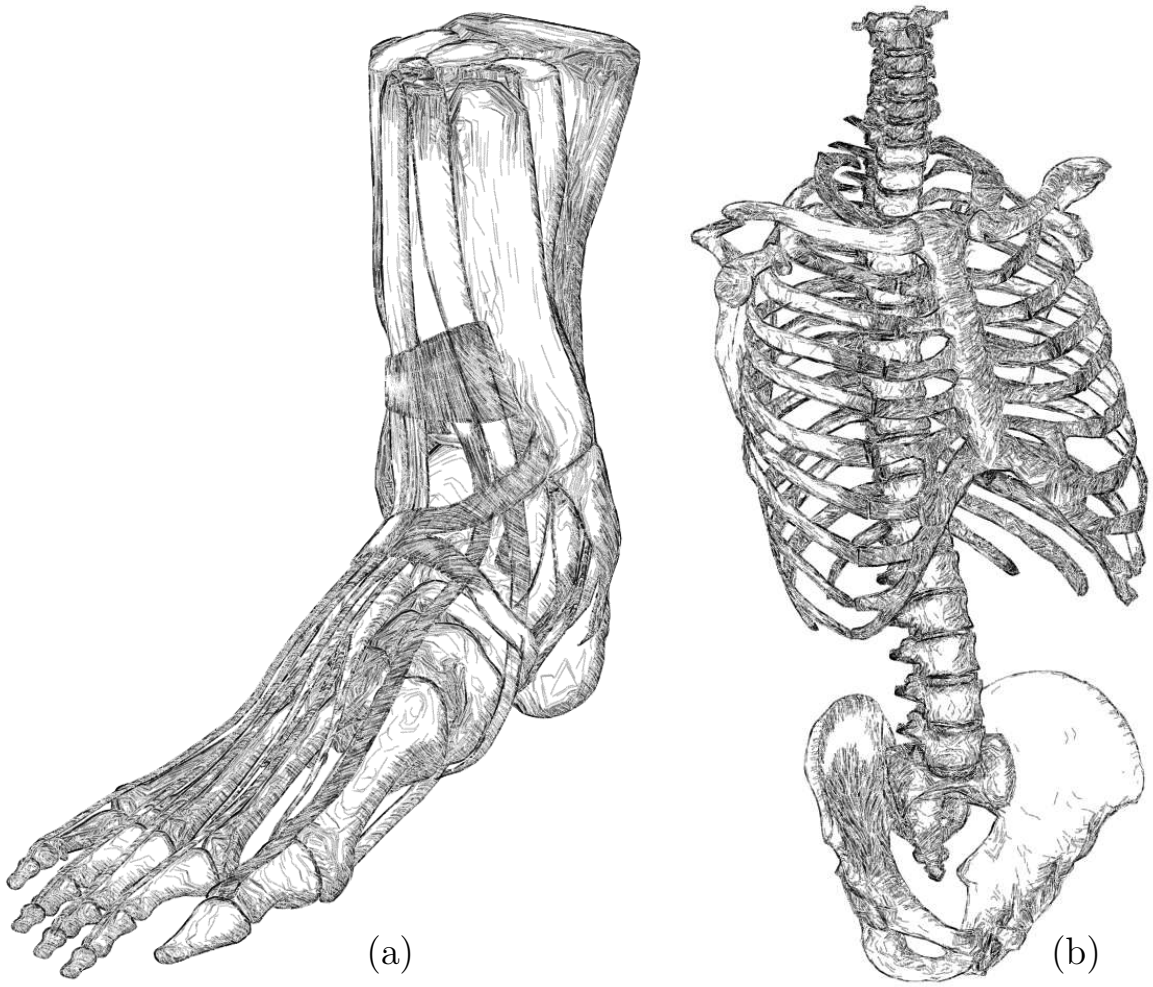

Fig. 11 Anatomical geometry of a human foot (a) and torso (b) rendered using Algorithm 1 with orthocline cosine shading strokes and isocline importance strokes.

augmented by cosine shading information to achieve the desired appealing final results.

The importance map derived by the approach proposed in this work might also be used in related applications and rendering styles. For example, following [4], our importance map could be directly used to control the opacity in NPR images.

Finally, we are in the process of exploring the use of modern hardware programming technologies, or programmable vertex shaders, toward importance-based line-art NPR rendering techniques.

6 Acknowledgment

The research was supported in part by the Fund for Promotion of Research at the Technion, Haifa, Israel, in part by the European FP6 NoE grant 506766 (AIM@SHAPE), and in part by the Israeli Ministry of Science Grant No. 01-01-01509.

We would like to thank Matthew Kaplan and Emil Saucen for their comments on various drafts of this work.

The models of the pony and the torso, are from 3dcafe, www.3dcafe.com. The model of the dinosaur is from Cyberware, http://www.cyberware.com/samples. The model of the armadillo is from the Stanford 3D scanning repository, http://www-graphics.stanford.edu/data/3Dscanrep. The face spline model is from Anath Fisher, ME, Technion. We are thankful to all. The model of David is part of The Digital Michelangelo Project (see http://graphics.stanford.edu/papers/dmich-sig00). We are thankful to Marc Levoy and Dave Koller for their aid in using this last dataset.

References

1. Benichou, F., and Elber, G. Output sensitive extraction of silhouettes from polygonal geometry. In *The Seventh Pacific Graphics 99, Seoul, Korea* (Oct. 1999), pp. 60–69.

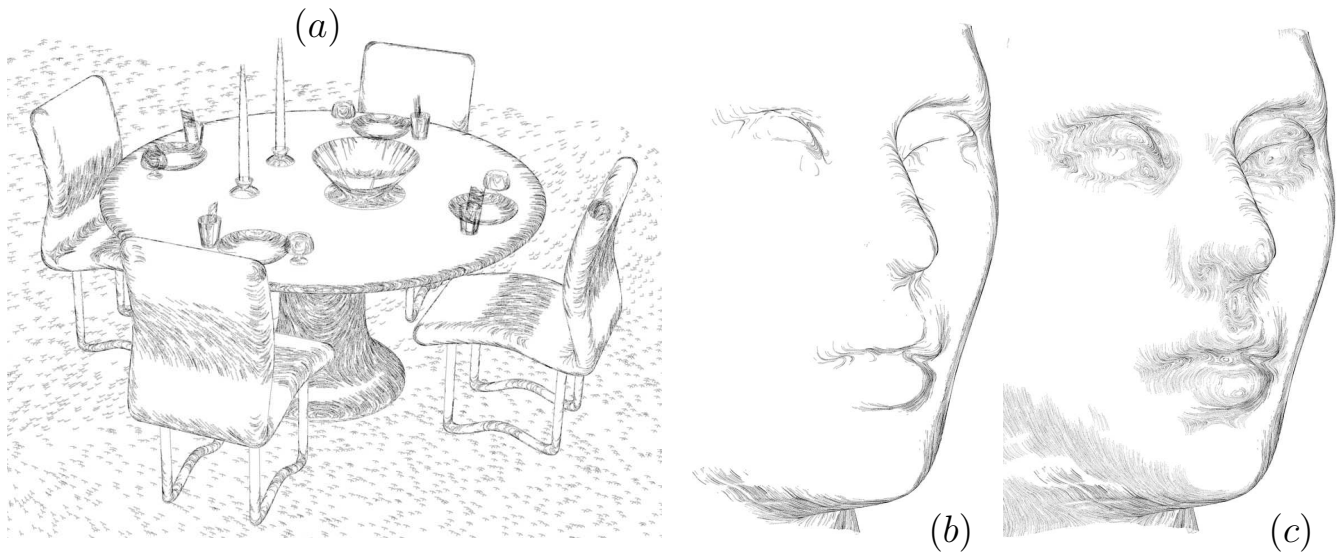

Fig. 12 Freeform NURBs scenes rendered directly using Algorithm 1 with orthocline cosine shading strokes and isocline importance strokes. The dinner scene in (a) consists of about forty freeform NURBs. The single bi-cubic NURBs surface face mask in (b) and (c) has a mesh size of 50×50. In (b), only silhouette strokes are shown whereas in (c) both silhouette and importance strokes are shown. All images were rendered with orthocline cosine shading strokes and isocline importance strokes.

2. Bremer, D. J., and Hughes, J. F. Rapid approximate silhouette rendering of implicit surfaces. In *Proc. of Implicit Surfaces '98* (1998), pp. 155–164.
3. DeCarlo, D., Finkelstein, A., Rusinkiewicz, S., and Santella., A. Suggestive contours for conveying shape. In *Computer Graphics (SIGGRAPH '03 Proceedings)* (Aug. 2003), pp. 848–855.
4. Diepstraten, J., Weiskopf, D., and Ertl., T. Transparency in interactive technical illustrations. *Computer Graphics Forum, Eurographics 2002 Conference Proceedings 21*, 3 (2002), 317–325.
5. DoCarmo, M. *Differential Geometry of Curves and Surfaces*. Prentice-Hall, 1976.
6. Elber, G. Interactive line art rendering of freeform surfaces. *Computer Graphics Forum, Eurographics 1999 Conference Proceedings 18*, 3 (Sept. 1999), 1–12.
7. Elber, G. Irit 9.5 user's manual, technion. *http://www.cs.technion.ac.il/∼irit* (Feb 2004).
8. Elber, G., and Cohen, E. Hidden curve removal for free form surfaces. In *Computer Graphics (SIGGRAPH '90 Proceedings)* (Aug. 1990), vol. 24, pp. 95–104.
9. Hilbert, D., and Cohn-Vossen, S. *Geometry and the Imagination*. Chelsea Publishing Company, 1952.
10. Hoschek, J., and Lasser, D. *Fundamentals of Computer Aided Geometric Design*. A. K. Peters, 1993. ISBN 1-56881-007-5.
11. Interrante, V. L. Illustrating surface shape in volume data via principal direction-driven 3D line integral convolution. In *SIGGRAPH 97 Conference Proceedings* (Aug. 1997), pp. 109–116.
12. Isenberg, T., Freudenberg, B., Halper, N., Schlechtweg, S., and Strothotte, T. A developer's guide to silhouette algorithms for polygonal models. *IEEE Computer Graphics and Applications 23*, 4 (July – Aug. 2003), 28–37.
13. Lu, A., Morris, C., Ebert, D., Rheingans, P., and Hansen, C. Non-photorealistic volume rendering using stippling techniques. In *IEEE Visualization 2002* (2002).
14. Markosian, L., Kowalski, M. A., Trychin, S. J., Bourdev, L. D., Goldstein, D., and Hughes, J. F. Real-time nonphotorealistic rendering. In *SIGGRAPH 97 Conference Proceedings* (Aug. 1997), pp. 415–420.
15. Meek, D., and Walton, D. On surface normal and gaussian curvature approximations given data sampled from a smooth surface. *Computer Aided Geometric Design 17* (2000), 521–543.
16. Plantinga, S., and Vegter, G. Contour generators of evolving implicit surfaces. In *Proc. of the 8th ACM Symposium on Solid Modeling and Applications* (June 2003), pp. 23–32.
17. Pop, M., Barequet, G., Duncan, C. A., and Goodrich, M. T. Efficient perspective-accurate silhouette computation. In *Proc. 17th Ann. ACM Symp. on Computational Geometry (SoCG)* (June 2001), pp. 60–68.
18. Raskar, R., and Cohen, M. Image precision silhouette edges. In *The Symposium on Interactive 3D Graphics* (1999), pp. 135–140.
19. Salisbury, M. P., Wong, M. T., Hughes, J. F., and Salesin, D. H. Orientable textures for image-based pen-and-ink illustration. In *SIGGRAPH '97: Proceedings of the 24th annual conference on Computer graphics and interactive techniques* (1997), pp. 401–406.
20. Sander, P. V., Gu, X., Gortler, S. J., Hoppe, H., and Snyder, J. Silhouette clipping. In *Computer Graphics (SIGGRAPH '00 Proceedings)* (July 2000), pp. 327–334.
21. Schein, S., and Elber, G. Adaptive extraction and visualization of silhouette curves from volumetric datasets. *The Visual Computer 20*, 4 (2004), 243–252.
22. Sousa, M. C., Foster, K., Wyvill, B., and Samavati, F. Precise ink drawing of 3d models. *Computer Graphics Forum, Eurographics 2003 Conference Proceedings 22*, 3 (2003), 369–379.
23. Sousa, M. C., and Prusinkiewicz, P. A few good lines: Suggestive drawing of 3d models. *Computer Graphics Forum, Eurographics 2003 Conference Proceedings 22*, 3 (2002), 381–390.
24. Thirion, J.-P., and Gourdon, A. Differential characteristics of isointensity surfaces. *Computer Vision and Image Understanding 61*, 2 (1995), 190–202.